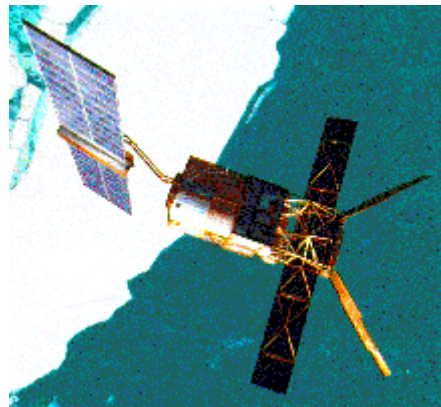

ERS-2 SAR CYCLIC REPORT

C Y C L E 9 5

18-MAY-2004 to 22-JUN-2004



Prepared by:	PCS SAR TEAM
Issue:	1.0
Reference:	
Date of Issue	
Status:	
Document type:	Technical Note
Approved by:	

T A B L E O F C O N T E N T S

1	INTRODUCTION	3
2	EXTERNAL CALIBRATION	4
2.1	ERS-2 TRANSPONDER MONITORING	4
3	ANTENNA PATTERN MONITORING	6
3.1	IMAGE MODE INTERNAL CALIBRATION	14
3.1.1	<i>High rate products analysis</i>	14
3.1.2	<i>QCP analysis</i>	16
3.2	WAVE MODE INTERNAL CALIBRATION	19
3.2.1	<i>Calibration pulse power monitoring</i>	19
4	SAR PERFORMANCE	22
4.1	IMAGE/WAVE ACQUISITION	22
4.2	DOPPLER/ATTITUDE ANALYSIS	22
4.2.1	<i>AOCS overview</i>	22
4.2.2	<i>Attitude monitoring</i>	23
4.2.3	<i>SAR high rate Doppler monitoring</i>	24
	ANNEX A: WAVE CALIBRATION PULSE POWER	25
	ANNEX B: PRODUCTS QUALITY ANALYSIS	26

1 INTRODUCTION

This document addresses the results of the analysis made on the ERS-2 SAR instrument for the cycle 95 concerning the following activities:

1. external calibration in section 2
2. antenna pattern monitoring in section 3. **Please note that the antenna pattern results are relative to the cycle 94. An update of the document is planned as soon as the data is available.**
3. internal calibration for High rate and Low bit rate mode in section 0
4. attitude/Doppler monitoring in section 4

For further information or comments please write to eohelp@esa.int.

2 EXTERNAL CALIBRATION ~~SAR CALIBRATION~~

External calibration is specific activity performed since the beginning of the ERS-2 mission in order to calibrate the instrument against ground target transponders with a known radar cross-section (RCS).

The SAR calibration site is Flevoland in The Netherlands (NL), with 3 transponders having the following coordinates:

Transponder	Latitude	Longitude
1: Pampushout	+52.36651429N	+5.15197438E
2: Lelystad	+52.45806341N	+5.52755628 ^E
3: Minderhout	+52.55502077N	+5.66896505 ^E

Table 1: Flevoland Transponders coordinates

2.1 ERS-2 Transponder monitoring

Please note that transponder 1 was last detected in 2 Feb 1997, and it has been no longer active ever since. Detection of point targets has continued on transponder 2 and 3, with alternating shuts off. Transponder 2 was last visible on 17 Oct 2001, and finally Transponder 3 was last visible on 22 Mar 2002.

From this date, there has been no detection of point targets in the designated areas in all the following NL scenes.

Date	Value	ERSTran2	ERSTran3	Aalsmeer	Edam
23/06/2000 10:34	Relative_rcs [dB]	0.551746			
	Measured_rcs [dB]	58.2417			
	K [dB]	120.603494			
19/07/2000 21:41	Relative_rcs [dB]		-0.189056		
	Measured_rcs [dB]		57.6609		
	K [dB]		119.121888		
28/07/2000 10:35	Relative_rcs [dB]	0.493343	0.170734		
	Measured_rcs [dB]	58.1833	58.0207		
	K [dB]	120.486688	119.84147		
01/09/2000 10:35	Relative_rcs [dB]	0.381512	0.165394		
	Measured_rcs [dB]	58.0715	58.0154		
	K [dB]	120.26302	119.830789		
10/11/2000 10:35	Relative_rcs [dB]	0.381512	-0.503609		

	Measured_rcs [dB]	58.0715	57.3464		
	K [dB]	120.263025	118.492784		
15/12/2000 10:35	Relative_rcs [dB]	0.46516	-0.050087		
	Measured_rcs [dB]	58.1552	57.7999		
	K [dB]	120.430322	119.399827		
25/04/2001 21:40	Relative_rcs [dB]		-0.370335		
	Measured_rcs [dB]		57.4797		
	K [dB]		118.759332		
04/05/2001 10:34	Relative_rcs [dB]	0.287502			
	Measured_rcs [dB]	57.9775			
	K [dB]	120.075006			
12/02/2003 10:36	Relative_rcs [dB]			-1.14894	
	Measured_rcs [dB]			60.2111	
	K [dB]			117.2021	
09/05/2003 10:33	Relative_rcs [dB]				-0.31983
	Measured_rcs [dB]				61.8902
	K [dB]				118.86

With:

$\text{relative_rcs[dB]} = \text{measured_rcs[dB]} - \text{nominal_RCS[dB]}$

$\text{K [dB]} = \text{relative_rcs[dB]} + \text{K annotated [dB]}$

3 ANTENNA PATTERN MONITORING

Please note that the antenna pattern results are relative to the cycle 93. An update of the document is planned as soon as the data is available.

The Amazon Rain-Forest (RF) presents a well-known and very stable backscattering characteristic. Its homogeneity and isotropic properties provide a stable and constant gamma nought allowing the SAR Antenna Pattern monitoring. SAR acquisitions in ascending and descending pass are acquired over (RF) to investigate changes in the antenna pattern.

Since transponders are no more available, acquisitions over the RF it also supports the radiometric stability analysis mainly based on transponders up to now.

The data will be acquired at the station of Cotopaxi (Ecuador) and Cuiaba (Brazil) and shipped to ESRIN/CPRF for processing.

The RF data analysis is performed each cycle for the previous one due to the time needed to process HR data, causing a delay in the images availability.

Seven images have been selected over this area for cycle 93; their characteristics are summarized in Table 2.

Scene	Orbit – Frame	Acquisition date	Centre lat/long (deg)	Mean σ_0 (dB)
1	46586 – 3735 (descending)	18-Mar-2004 14:42:48.025	Lat: -6.3610 Lon: 292.7720	-6.878
2	46586 - 3753 (descending)	18-Mar-2004 14:43:03.102	Lat: -7.2550 Lon: 292.5730	-6.880
3	46593 - 7047 (ascending)	19-Mar-2004 03:13:16.040	Lat: -7.0790 Lon: 292.5660	-6.724
4	46593 - 7065 (ascending)	19-Mar-2004 03:13:31.108	Lat: -6.1850 Lon: 292.3670	-6.695
5	46815 – 3735 (descending)	03-Apr-2004 14:39:56.062	Lat: -6.3590 Lon: 293.4940	-6.851
6	46815 – 3753 (descending)	03-Apr-2004 14:40:11.108	Lat: -7.2510 Lon: 293.2950	-6.831
7	46822 – 7065 (ascending)	04-Apr-2004 03:10:39.711	Lat: -6.1670 Lon: 293.0870	-6.806

Table 2: Selected Rain Forest scenes for cycle 94

Non-uniform regions have been masked in order to perform the antenna pattern monitoring. Some results of the analysis over the selected scenes are reported in the figures below.

The antenna patterns derived from the selected scenes are shown in Figure 1 and Figure 2 for descending and ascending passes respectively; Figure 3 and Figure 4 show the combination of the patterns for the available scenes, with the current VMP antenna pattern and their difference overplotted.

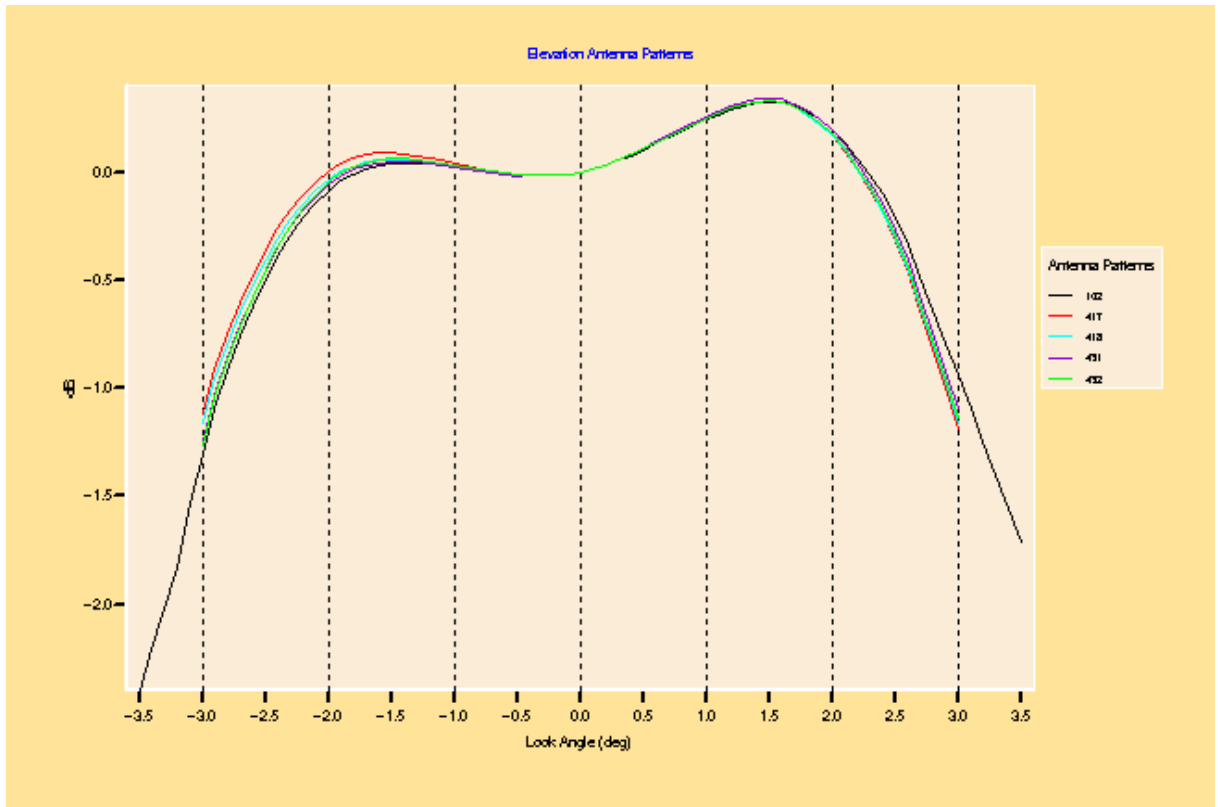


Figure 1: Antenna patterns derived from the selected descending pass plus reference pattern (in black)

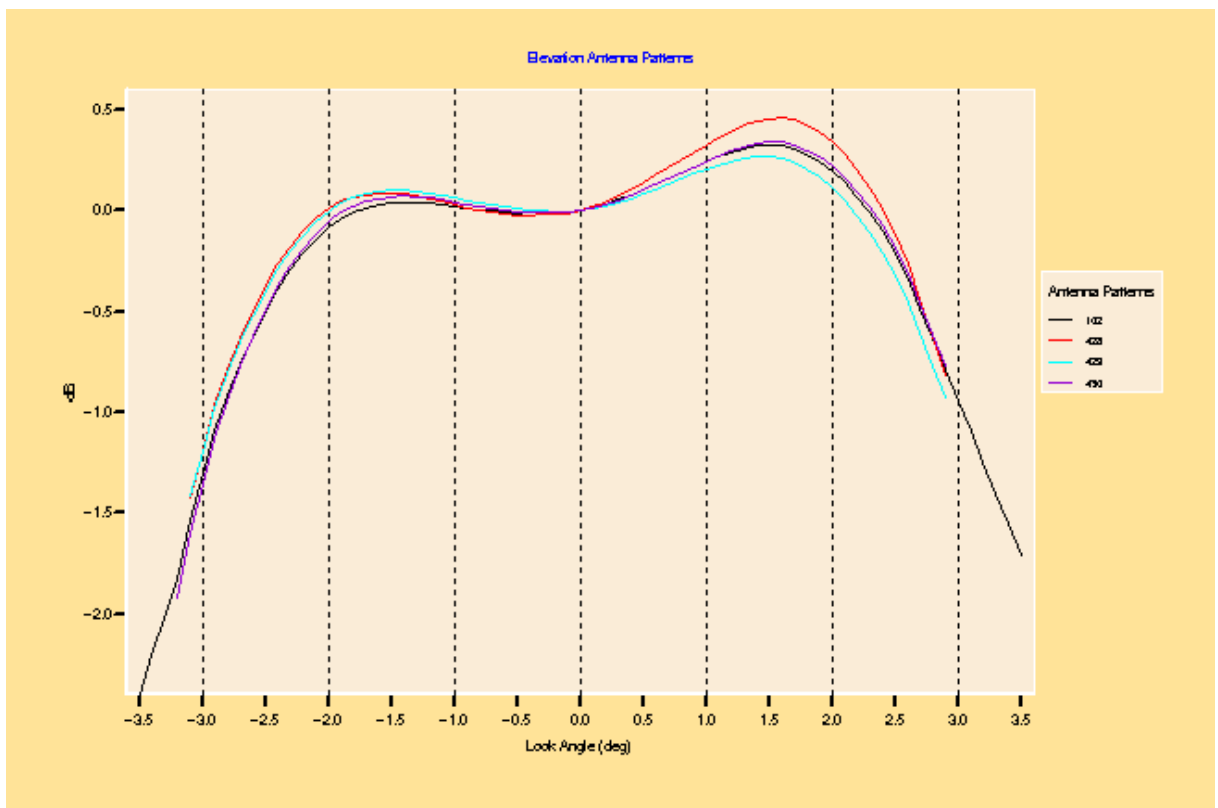


Figure 2: Antenna patterns derived from the selected ascending passes plus reference pattern (in black)

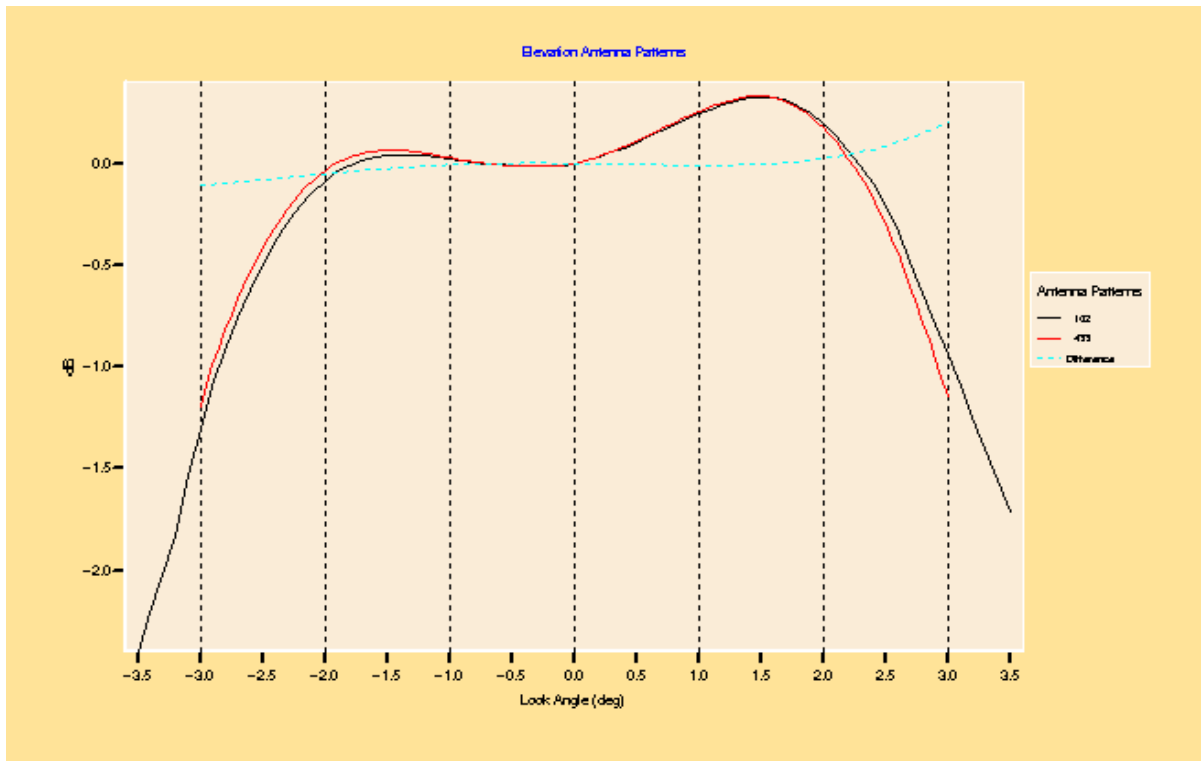


Figure 3: Antenna pattern combination (red curve) plus reference pattern (black curve) plus difference (blue curve) for descending passes

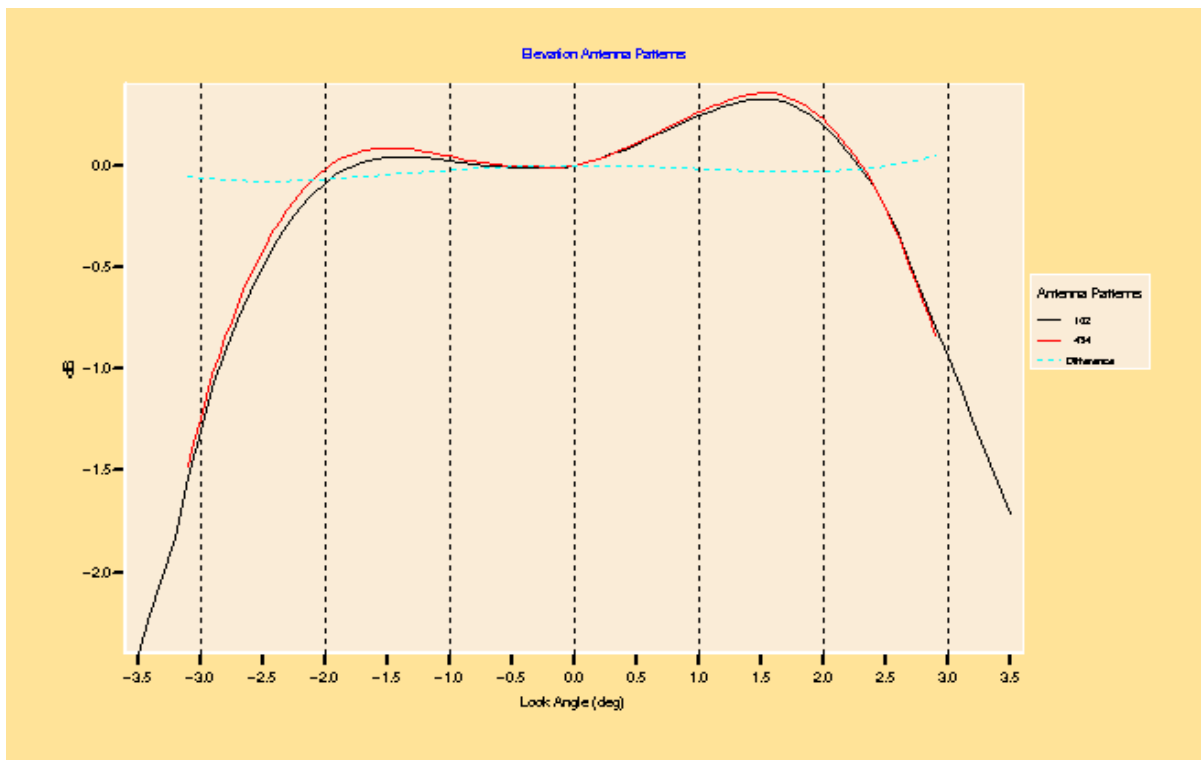
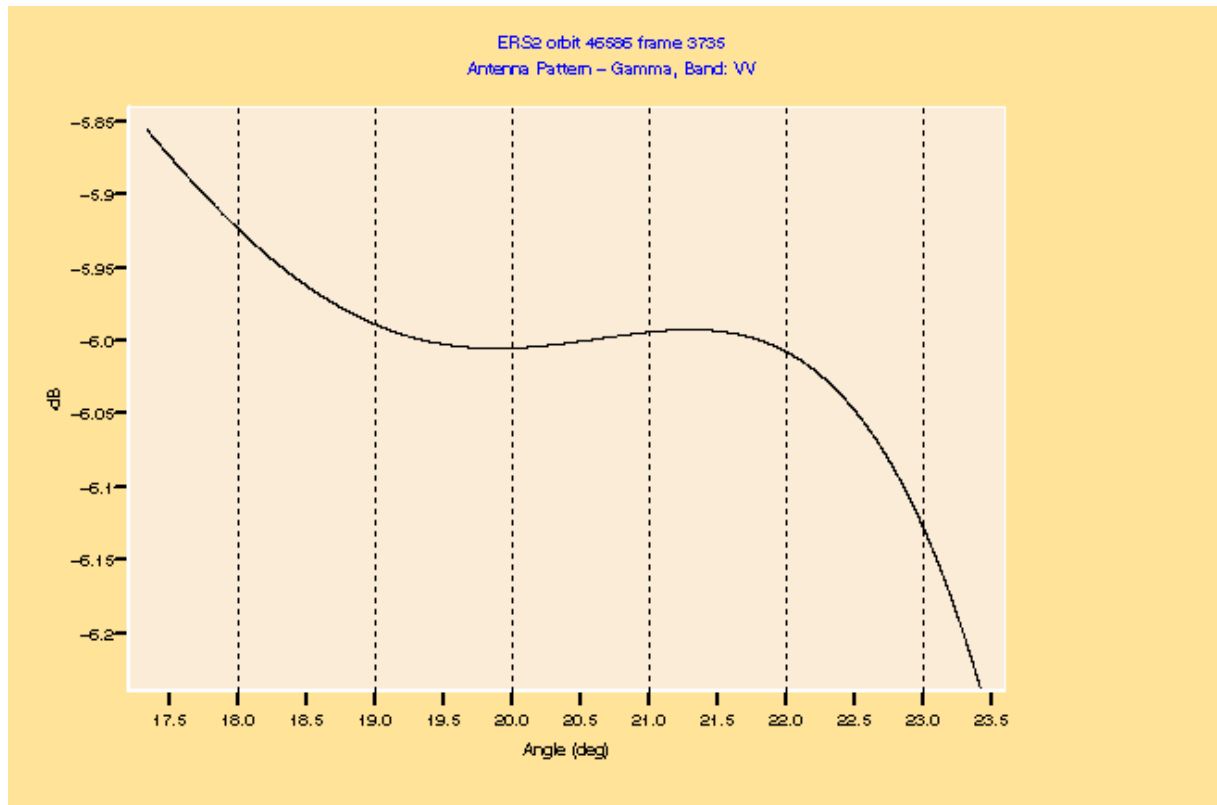
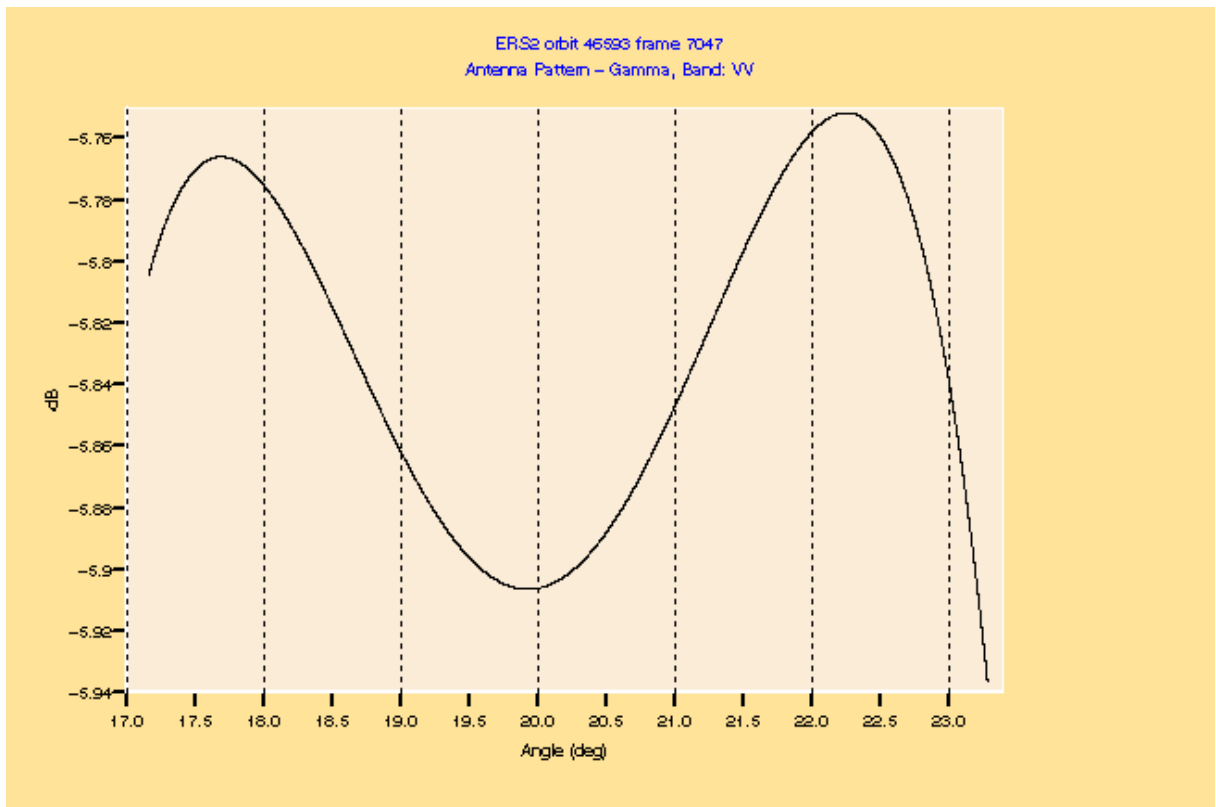
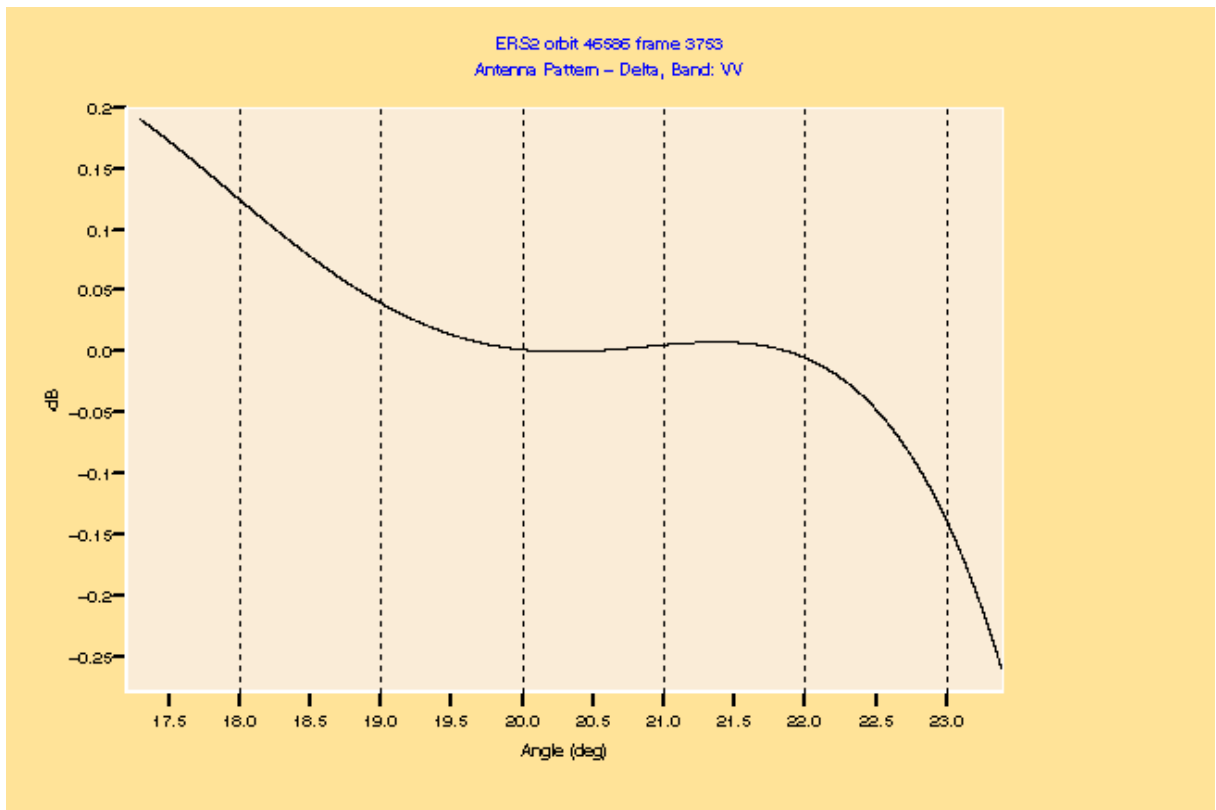


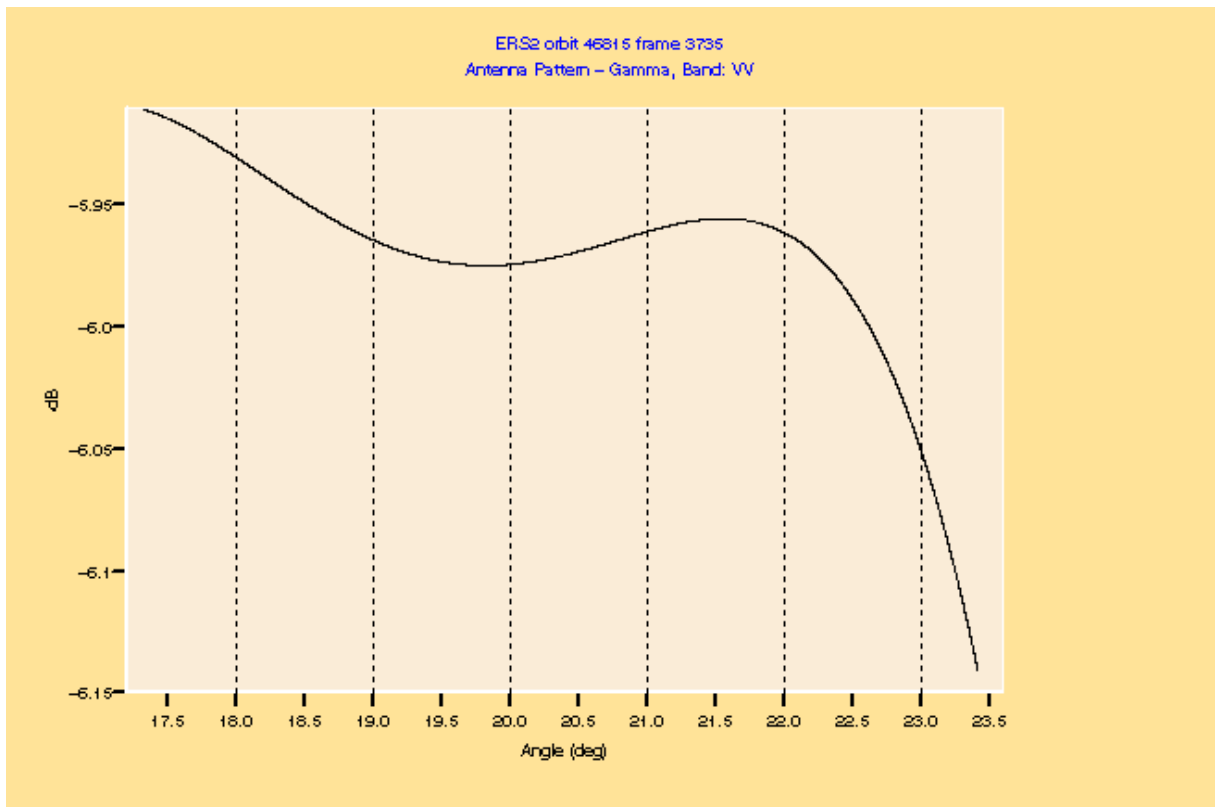
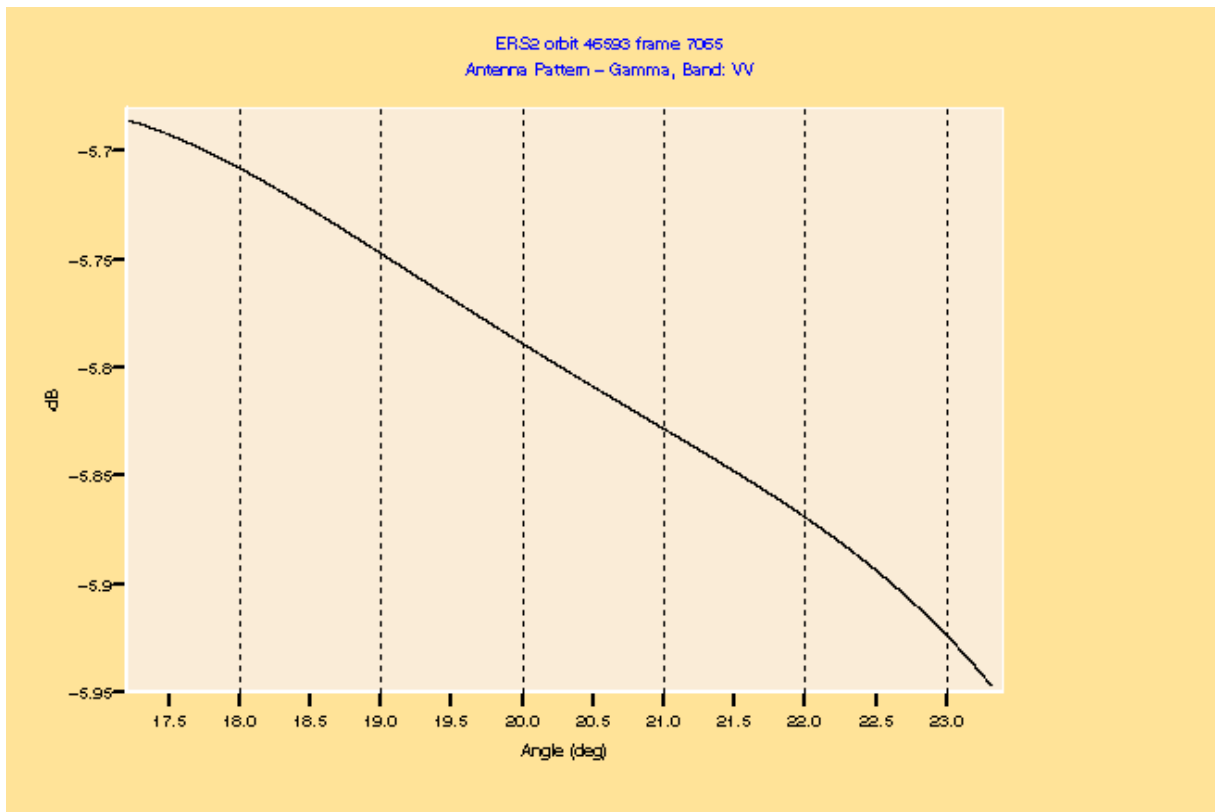
Figure 4: Antenna pattern combination (red curve) plus reference pattern (black curve) plus difference (blue curve) for ascending passes

The gamma profile for each selected scene is shown in the figures below.

~~The delta gamma absolute value is low for the analysed scenes, showing a good approximation of the actual antenna pattern.~~ The absolute calibration has been checked referring the mean gamma value, reported in Table 3. It's around 6.6/6.7 dB for the selected scenes, so quite close to the nominal value (6.5 dB for this area).







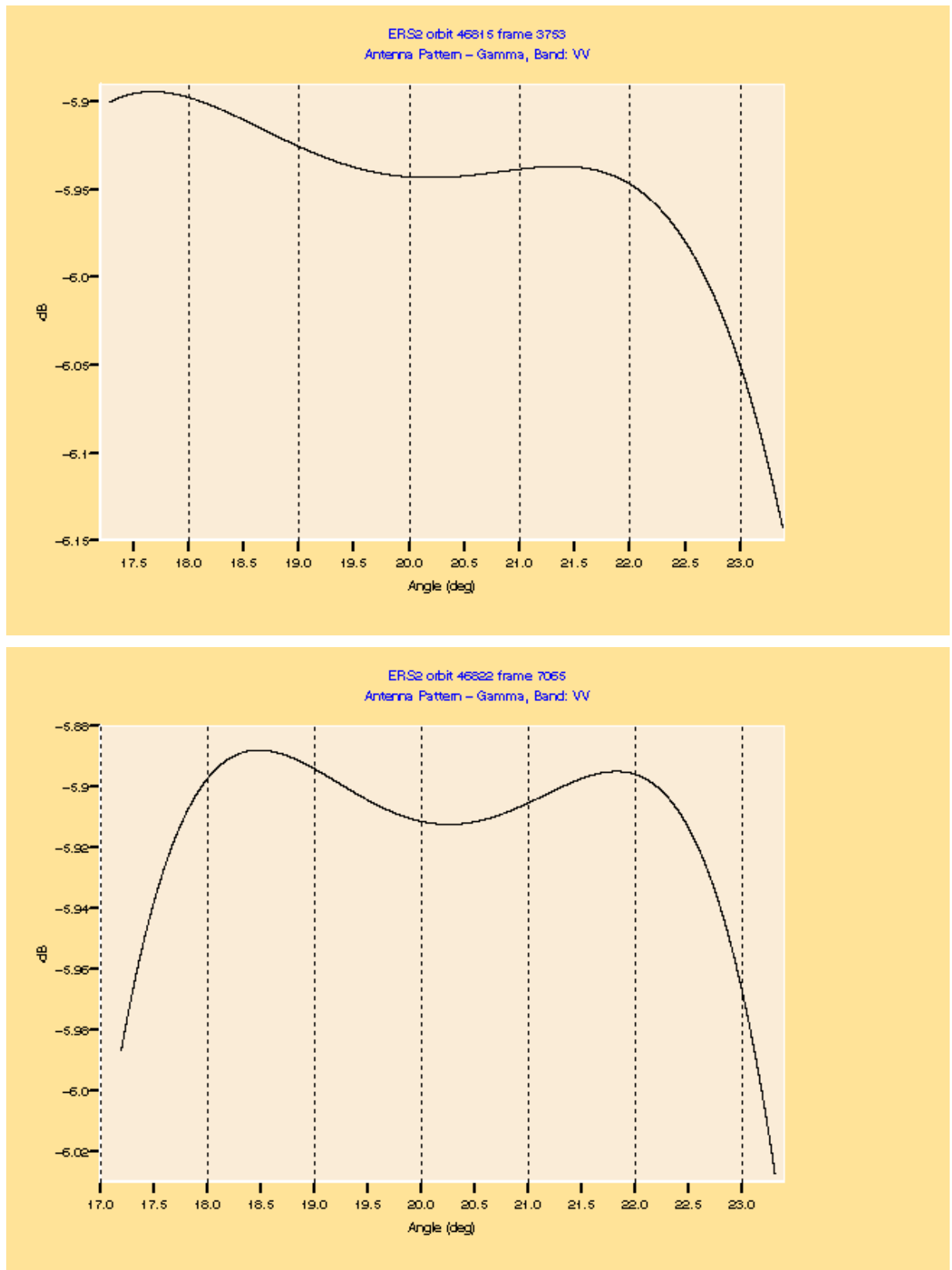


Figure 5: Gamma profiles for the available scenes

Scene	Orbit – Frame	Mean gamma (dB)
1	46586 – 3735 (descending)	-6.520
2	46586 - 3753 (descending)	-6.523
3	46593 - 7047 (ascending)	-6.369
4	46593 - 7065 (ascending)	-6.339
5	46815 – 3735 (descending)	-6.493
6	46815 – 3753 (descending)	-6.474
7	46822 – 7065 (ascending)	-6.450

Table 3: Mean gamma value for the selected scenes

Internal calibration

3.1 Image mode internal calibration

During the cycle 82, a gain increase of 3.5dB has been performed in two steps:

- Increase of the Image up-converter level by 2.5dB on 26 February 2003.
- Decrease of the Image receiver attenuation gain by 1dB on 28 February 2003.

3.1.1 High rate products analysis

3.1.1.1 Replica pulse power monitoring

The replica pulse power is extracted from the annotations of the level 1 High Rate SLC and PRI products. As shown in the following plot, the replica pulse power has lost ~5dB since the beginning of the mission with a regular slope of -0.57 dB/year until the gain increase of 3.5B performed in February 2003. Figure 6 shows that the calibration pulse power has retrieved the level of May 1998. Since the gain increase, the replica pulse power is decreasing with a slope of -0.172 dB/Cycle.

Figure 7 shows the evolution of the HR calibration pulses during the current cycle. Please note the very regular evolution of the power level, which is concordant with the QCP analysis. For the current cycle, the calibration pulse level has reached a mean value of 50.38dB. Please note that for the current cycle, very few QCP data were available.

Table 4 gives the replica pulse power correction factor averaged over 3 months.

Year	Jan-Feb-Mar	Apr-May-Jun	Jul-Aug-Sep	Oct-Nov-Dec
1995	Not available	Not available	215.23	210.835
1996	203.534	201.705	196.501	184.085
1997	178.818	173.012	164.666	159.916
1998	155.797	150.462	146.509	140.186
1999	139.446	133.889	132.352	129.449
2000	127.202	121.463	120.669	115.158
2001	110.416	109.128	99.859	98.068
2002	91.014	93.22	86.05	82.954
2003	76.578 /151.28	153.464	153.805	148.575
2004	146.281	149.892	147.715	Not available

Table 4: Evolution of Replica Pulse Power correction factor from the HR products. The yellow case is relative to the gain increase of March 2003

3.1.2 QCP analysis

As a replacement of the UIND¹ and UIC² products, the QCP files are used to monitor the evolution of the:

- replica pulse power,
- calibration pulse power and
- noise power (not calibrated)

In particular, QCP gives two measures of the above parameters: at the start/end of the acquisition. For further details on QCP, please see annex B. Please see Figure 8 for trend plots where red points are for the measures at the beginning of the product and green are the ones at the end.

1. Replica Pulse Power

The replica pulse power measurements (start/stop) are almost identical. Since the gain increase, the level decreases with a slope -0.54dB/year . For the current cycle the power level reaches a mean level of 49.52dB . As done previously with the HR products, the mean replica pulse power derived from the QCP is given in Table 5.

2. Calibration Pulse Power

As the measure made at the end of the segment is noisier, only the first measure is used. For the current cycle the power level has reached a mean level of 43.42dB . As shown in Figure 9 there is (as expected) a linear correlation between replica and calibration pulse power. Since the gain increase, the mean calibration pulse power is decreasing with a regular slope of -0.492dB/year .

¹ UIND gives information on noise power level and the calibration pulse power level

² UIC gives on the replica Pulse power

3. Noise Power

The noise power level seems to be constant during the whole mission. It decreases with a low slope of -0.04dB/year from the last gain increase. During the current cycle it has reached a mean level of 7.49dB .

Year	Jan-Feb-Mar	Apr-May-Jun	Jul-Aug-Sep	Oct-Nov-Dec
1996	211.622	205.018	Not available	184.384
1997	182.15	173.055	167.219	162.305
1998	155.998	151.48	144.595	138.553
1999	135.867	128.822	Not available	127.188
2000	115.325	109.939	109.38	105.205
2001	101.302	97.039	91.881	88.518
2002	83.486	81.575	77.354	72.151
2003	70.864/145.35	139.799	134.951	129.152
2004	122.444	123.601	121.708	Not available

Table 5: Evolution of Replica Pulse correction factor for QCP files. The yellow case is relative to the gain increase of March 2003

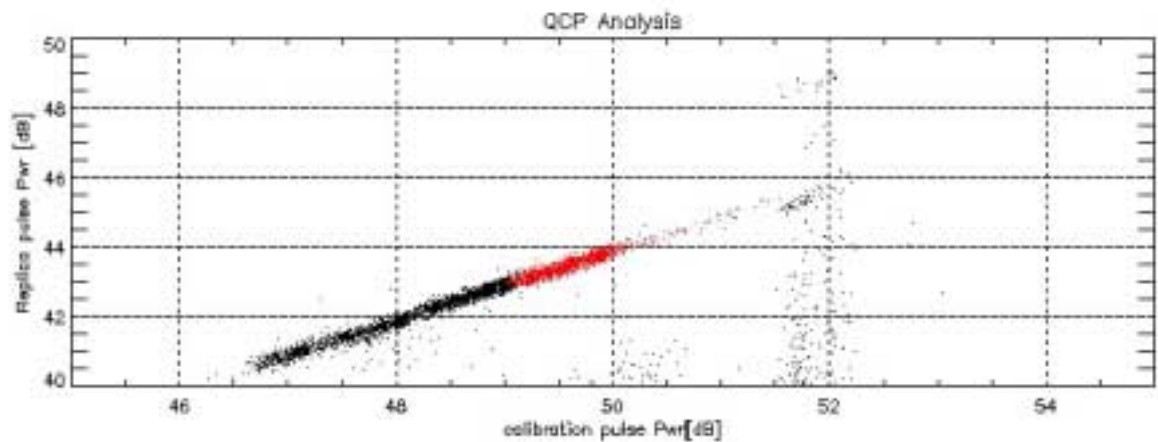


Figure 9: Joint evolution of Replica and calibration pulses. Black dots represent all the data since. Red ones are the data since the last gain increase.

3.2 Wave mode internal calibration

3.2.1 Calibration pulse power monitoring

From cycle 39 to 77 (Jan-1999 to Sep-2002), the calibration pulse power was decreasing with a slope of -0.215dB/year .

On 4th September 2002 an update of the ERS-2 AMI up-converter gain occurred. For wave mode the gain was increased by 3dB. However, only a change of $\sim 1\text{dB}$ has been measured, as shown in Figure 10. The level of the calibration pulse power rose up from 23.5dB to 24.4dB. Since the gain increase, the power level is decreasing with a regular slope of -0.228dB/year .

The calibration pulse power has reached for the current cycle a mean level of 24.10dB as show in Figure 11.

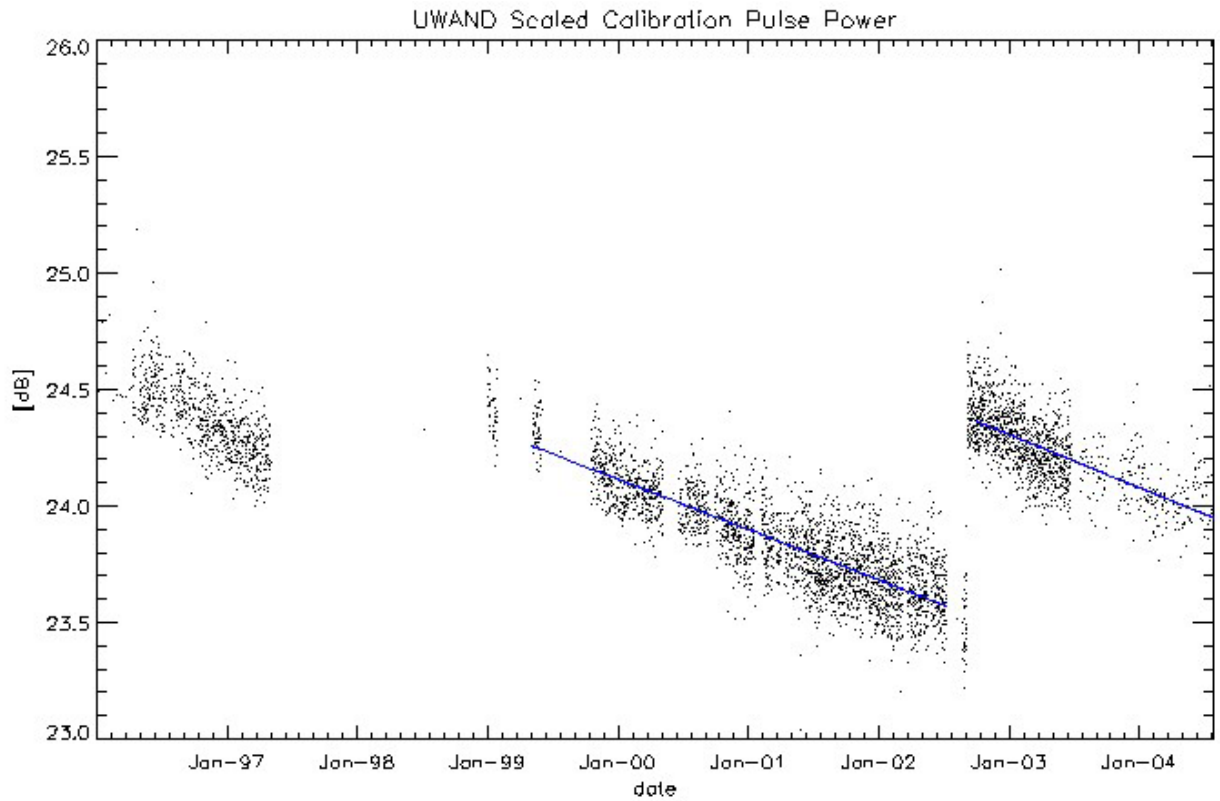


Figure 10: Evolution of Mean Calibration Pulse

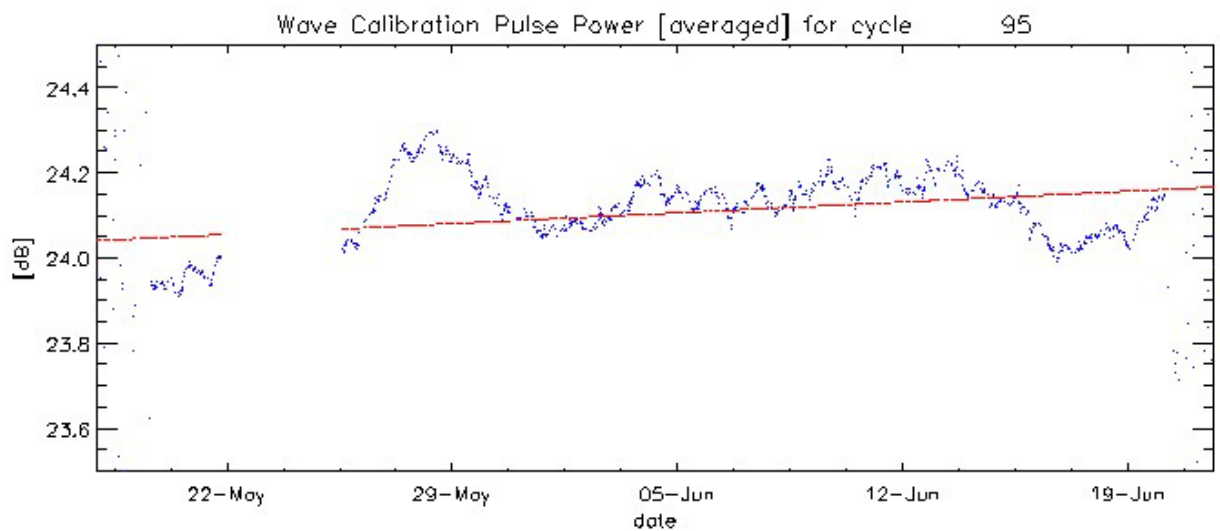


Figure 11: Evolution of Mean Calibration Pulse Power since for the current cycle



Please see appendix A for further details on calibration pulse power.

4 SAR PERFORMANCE

4.1 Image/Wave acquisition

Starting from July 2003, due to tape recorders failure, the ERS LR mission continues within the full coverage of ESA LBR receiving stations, which are:

- Maspalomas, Gatineau, Prince Albert, Kiruna: immediately available
- West Freugh, Matera, O'Higgins: available in the near future

Please note that SAR HR mission is not affected. By consequence, SAR image availability is not influenced.

4.2 Doppler/Attitude analysis

4.2.1 AOCS overview

ERS-2 was piloted in yaw-steering mode using three gyroscopes since the beginning of the mission until February 2000, when a new yaw-steering mode using only one gyroscope was implemented. The ERS-2 gyroscopes have experienced several problems during the mission and the new mono-gyro mode (1GP) was intended to ensure the mission continuity even in case of additional failures. In January 2001 a new test piloting mode using no gyroscopes, the Extra-Backup Mode (EBM), was implemented as a first stage of a gyro-less piloting mode. The aim of this challenging mode was to maintain the remaining gyroscopes performance only for those activities absolutely requiring them, such as some orbit maneuvers. A more accurate version of this yaw-steering zero-gyro mode (ZGM) was operationally used since June 2001 and the performance was further improved with the implementation of the Yaw Control Monitoring mode (YCM) at the beginning of 2002. The evolution from the nominal and extremely stable three-gyro piloting mode (3GP) to the YCM has allowed to successfully continuing the ERS-2 operations despite of the gyroscopes failures. Nevertheless, this evolution has significantly affected the stability of the satellite attitude and the SAR Doppler Centroid frequency. Figure 12 gives a summary of the ERS-2 piloting modes.

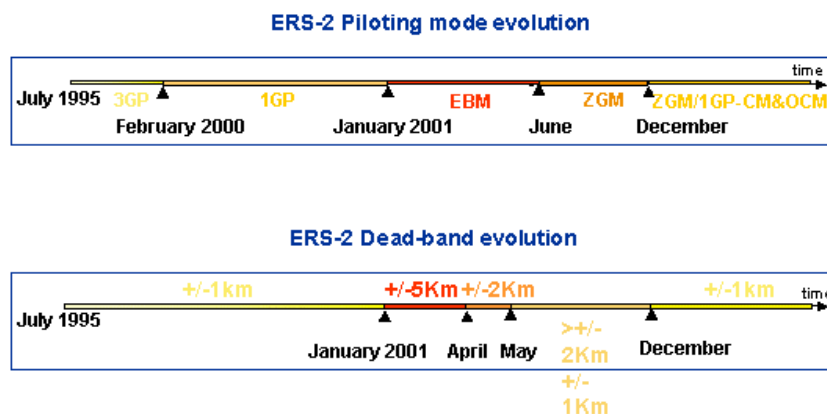


Figure 12: Summary of ERS-2 Piloting Mode

As an example of the attitude instability Figure 13 shows the evolution of the Doppler Centroid since the beginning of the ERS-2 mission.

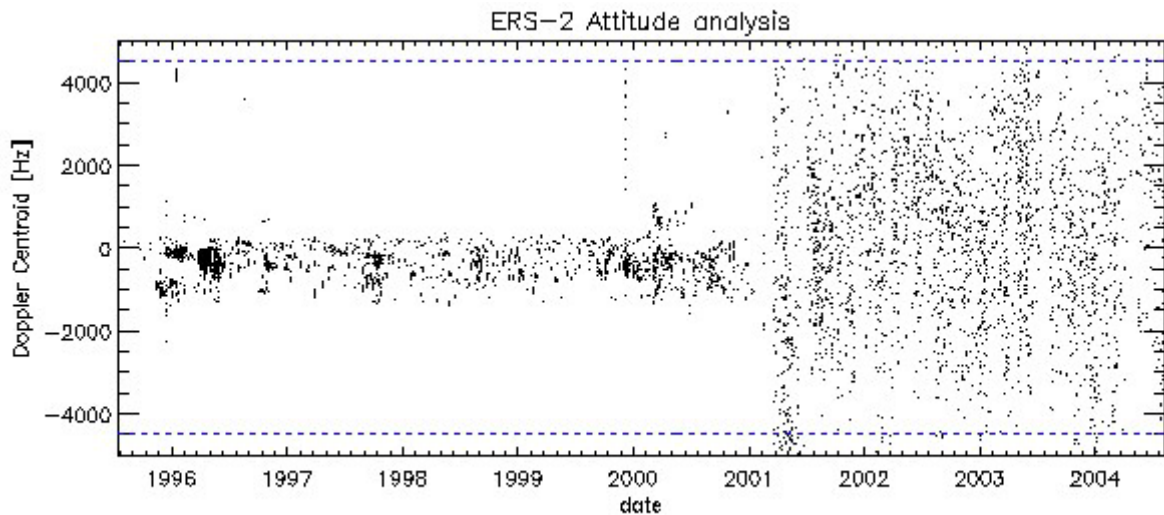


Figure 13: Evolution of Doppler Centroid Frequency since the beginning of the mission

4.2.2 Attitude monitoring

The YCM piloting mode requires a monitoring in near real time of the yaw angle. The mean yaw per orbit angle is currently derived from the wave data but will be replaced very soon by the HEY (scatt) measures.

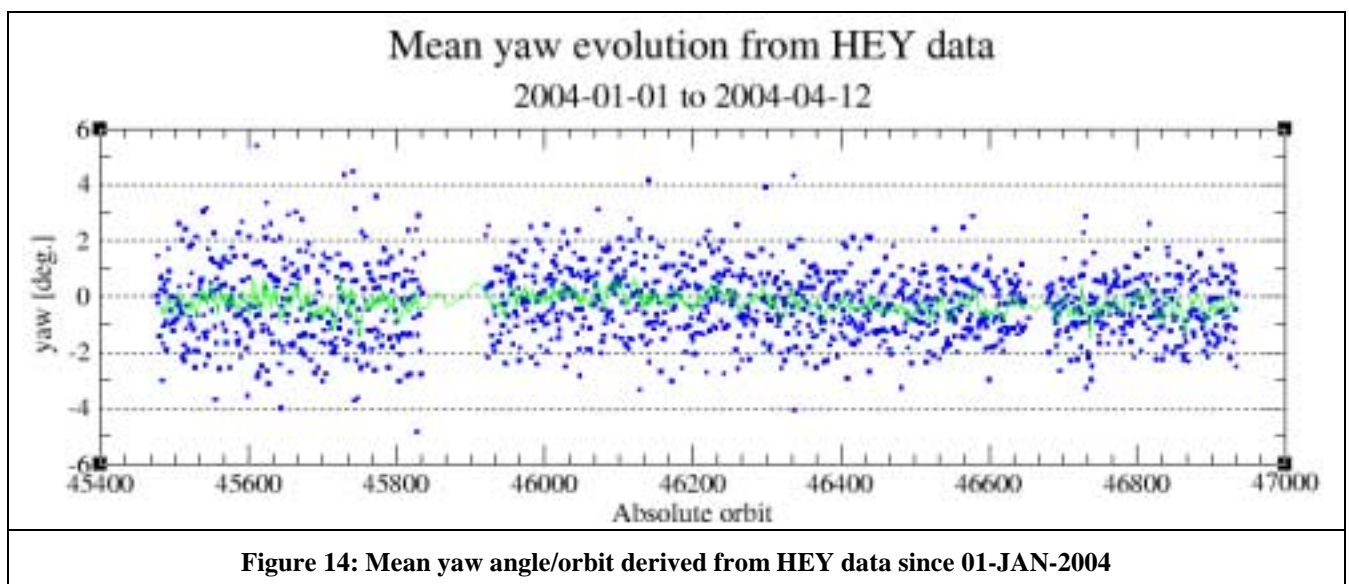


Figure 14: Mean yaw angle/orbit derived from HEY data since 01-JAN-2004

The mean yaw per orbit is most of the time constrain between ± 2 deg. For the current cycle the yaw angle has a bias of -0.38 deg with a deviation 1.04 deg.

4.2.3 SAR high rate Doppler monitoring

For monitoring purposes a specific HR product ordering (~90 products per cycle) is made to follow the evolution of the platform attitude/Doppler Centroid frequency.

For the current cycle 89% of the analyzed products have a Doppler centroid within ± 4500 Hz. However the dispersion over a same orbit position is representative of an attitude instability relative to a very high yaw variation, visible in Figure 15. In particular scenes on the last part of the orbit present a very high Doppler instability.

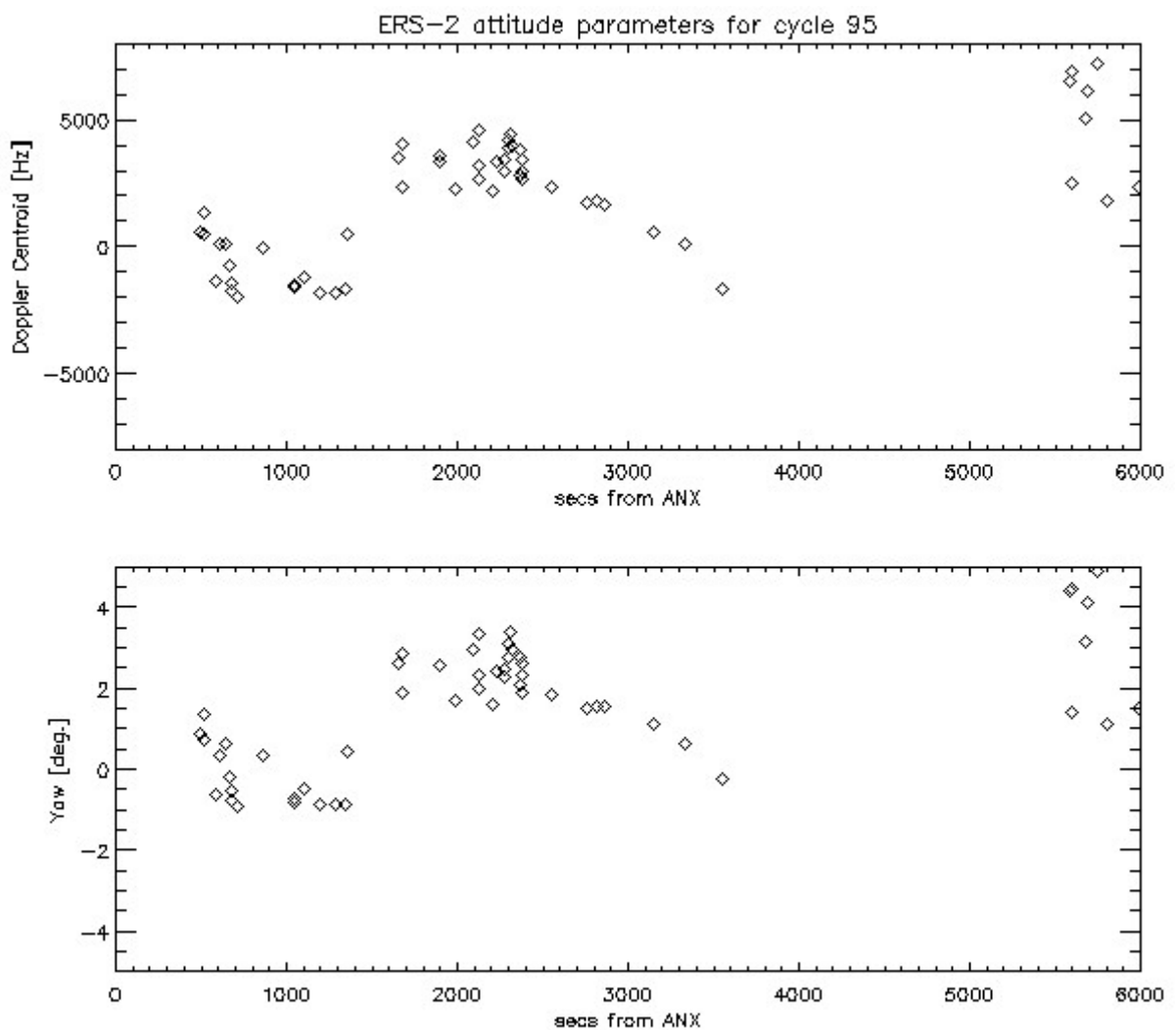


Figure 15: SAR HR Doppler Centroid evolution in time for versus seconds from ANX

ANNEX A: WAVE CALIBRATION PULSE POWER

Noise power density, scaled and unscaled calibration pulse power can be calculated extracting the following parameters from **UWAND** products:

- σ_I the standard deviation of I part noise data on SPH
- σ_Q the standard deviation of Q part noise data on SPH
- I and Q part of the 4 calibration pulse datasets

Noise power density

The noise power density is defined as follows:

$$npd = \sigma_I^2 + \sigma_Q^2$$

Calibration pulse power

For each four DSRs, we search the peak intensity of the calibration pulses. In order to take into account only the energy of the main lobe of the calibration pulses only 16 samples are used around the peak. If p is the position of the peak the calibration pulse power for one DSR is defined as following:

$$powerDSR = \frac{1}{16} \sum_{n=p-8}^{p+7} I_n^2 + Q_n^2$$

The Calibration Pulse Power is obtained by averaging:

$$CalibrationPulsePower = \frac{1}{4} \sum_{j=1}^4 powerDSR(j)$$

- a) Unscaled calibration pulse power

The unscaled calibration power is identical as the previous formula:

$$UnscaledCalibrationPulsePower = CalibrationPulsePower = \frac{1}{4} \sum_{j=1}^4 powerDSR(j)$$

- b) Scaled calibration pulse power

The scaled calibration pulse power is defined as follows:

$$scaledCalibrationPulsePower = CalibrationPulsePower - 16 * npd = \left[\frac{1}{4} \sum_{j=1}^4 powerDSR(j) \right] - 16 * npd$$

ANNEX B: PRODUCTS QUALITY ANALYSIS

This activity is principally dedicated to the user support. The two main types of activities are:

- Verification of products with a high Doppler value (rejected products)
- Product quality/format anomalies

Rejected products during the cycle

Rejected products are those having Doppler Centroid frequencies outside the interval $[-4500, 4500]$ Hz. In this case VMP ambiguity estimation is not reliable so the product's focusing has to be checked.

Product quality anomalies

Products quality anomalies are detected internally or via the users complaints. The action is to analyze the faulty products and report the analysis results.

Annex C: Example of QCP file

Processing - ERS_2_\$QCP200_027387.\$EXCHANGE

Filename = ERS_2_\$QCP200_027387.\$EXCHANGE
 File size in bytes = 3551
 Time of last access = 01-NOV-2002 19:33:37.000
 Time of last data modification = 27-JUL-2000 09:38:23.000
 Time of last file status change = 27-JUL-2000 09:38:23.000

[QCP200Header]

Filename = ERS_2_\$QCP200_027387.\$EXCHANGE
 ArrivalTime = 2000-07-27 09:38:23
 Platform Id = 2
 NumOfPasses = 1
 PassId = 1
 NumOfImagingSeqs = 1

[ImageSeqId_1]

NumberOfValidNoisePulsesStart = 3
 NumberOfValidCalibPulsesStart = 4
 NumberOfValidRepPulsesStart = 8
 MeanPowerOfValidRepStart = 78166.750000
 MeanPowerOfValidRepFlagStart = 0.000000
 IndexOfFirstValidRepSampleWindowStart = 29
 FirstValidReplicaSampleWindowFlagStart = 1
 RangeCompressionNormFactorStart = 77990.000000
 RangeCompressionNormFactorFlagStart = 0
 MeanPowerOfValidCalibStart = 18861.839990
 MeanPowerOfValidCalibFlagStart = 0
 MeanPowerOfValidNoiseStart = 5.681800
 MeanPowerOfValidNoiseFlagStart = 1
 NumberOfValidNoisePulsesEnd = 6
 NumberOfValidCalibPulsesEnd = 4
 NumberOfValidRepPulsesEnd = 8
 MeanPowerOfValidReplicaEnd = 77995.250000
 MeanPowerOfValidReplicaFlagEnd = 0
 IndexOfFirstValidReplicaSampleWindowEnd = 28
 FirstValidReplicaSampleWindowFlagEnd = 1
 RangeCompressionNormFactorEnd = 77890.000000
 RangeCompressionNormFactorFlagEnd = 0
 MeanPowerOfValidCalibEnd = 18015.237350
 MeanPowerOfValidCalibFlagEnd = 0
 MeanPowerOfValidNoiseEnd = 5.276930
 MeanPowerOfValidNoiseFlagEnd = 1
 MeanReplicaPulsePowerUpperThreshold = 255000.000000
 MeanReplicaPulsePowerLowerThreshold = 85000.000000
 MeanNoiseSignalPowerUpperThreshold = 7.500000
 MeanNoiseSignalPowerLowerThreshold = 2.500000
 MeanCalibSignalPowerUpperThreshold = 3750.000000
 MeanCalibSignalPowerLowerThreshold = 1250.000000
 RangeCompressNormFactorUpperThreshold = 255000.000000
 RangeCompressNormFactorLowerThreshold = 85000.000000